

## Binding of *meso*-Tetrakis(*N*-methylpyridium-4-yl)porphyrin to Triplex Oligonucleotides: Evidence for the Porphyrin Stacking in the Major Groove

Young-Ae Lee,<sup>†</sup> Jin-Ok Kim,<sup>†</sup> Tae-Sub Cho,<sup>†</sup> Rita Song,<sup>‡</sup> and Seog K. Kim<sup>\*,†</sup>

*Department of Chemistry, Yeungnam University, Dae-dong, Kyongsan City, Kyoung-buk 712-749, Republic of Korea, and Life Sciences Division, Korea Institute of Science and Technology, Seoul 136-791, Republic of Korea*

Received February 5, 2003; E-mail: seogkim@yu.ac.kr

Understanding the interaction between porphyrin and DNA is important due to its potential biological applications in photodynamic therapy, and for its unique DNA binding property.<sup>1</sup> The most extensively studied DNA binding porphyrin is cationic *meso*-tetrakis(*N*-methylpyridium-4-yl)porphyrin (TMPyP, Figure 1, inset). At low [TMPyP]/[DNA] ratios, the groove binding mode<sup>2,3</sup> and intercalation<sup>4</sup> have been suggested for the TMPyP complexed, respectively, with the AT and GC site of DNA. In the groove binding mode, whether the crescent-shaped side of TMPyP fits into the minor groove or it binds near the minor groove is still unclear, while porphyrins intercalate between the base pairs in the 5'CG3' site.<sup>4</sup> As the ratio increases, the outside binding mode, represented by a bisignate excitonic CD in the Soret region, dominates for both AT- and GC-rich DNAs.<sup>3,5</sup> However, the exact location of porphyrin that assembled (or stacked) outside of the AT and GC template still needs to be clarified.

In the poly(dA)·poly(dT)]<sub>2</sub> and poly(dG)·poly(dC)·poly(dC)<sup>+</sup> triple helical DNA, thymines and protonated cytosines, which are located in the major groove, block the binding of the major groove binding drugs or alter their binding properties.<sup>6</sup> On the other hand, the effect of the third strand on the binding mode of the minor groove binding drugs and intercalators is very small.<sup>7</sup> This concept was applied to this work: it was assumed that if porphyrin is located in the major groove of the duplex, the spectral property is expected to be altered to a great extent as compared to that assembled in the triplex, while if it is located near the minor groove, the spectral property would remain.

Figure 1 shows induced CD spectra in the Soret band of TMPyP in the presence of the d(A)<sub>12</sub>·d(T)<sub>12</sub> duplex and d(A)<sub>12</sub>·[d(T)<sub>12</sub>]<sub>2</sub> triplex. Here, the concentration, [oligonucleotide], indicates the concentration for the whole oligonucleotide. Therefore, 5 μM oligonucleotide indicates 60 base pairs (for duplex) or base triplets (for triplex). The triplex was stabilized by 1 mM Mg<sup>2+</sup>. The presence of Mg<sup>2+</sup> ions, in the absence of oligonucleotides, did not alter the absorption spectrum of TMPyP. Because the CD spectrum of the porphyrin–polynucleotide mixture is sensitive to the order of mixing and the concentration of NaCl,<sup>8</sup> the salt concentration was carefully controlled, and aliquots of a small volume of TMPyP were always added last. At a low [TMPyP]/[oligonucleotide] ratio (ratio lower than 0.4), which corresponds to 0.033 TMPyP molecule per base pairs (or base triplets), the CD spectrum shows a positive band at 425 nm with a shoulder in the 390–420 nm region, for both the duplex–TMPyP and the triplex–TMPyP complexes. The intensities of the CD spectra are similar. This result indicates that TMPyP binds either to the minor groove of both the duplex and the triplex or near the minor groove at these low mixing ratios. As the mixing ratio increases, a negative band at 434 nm and a positive

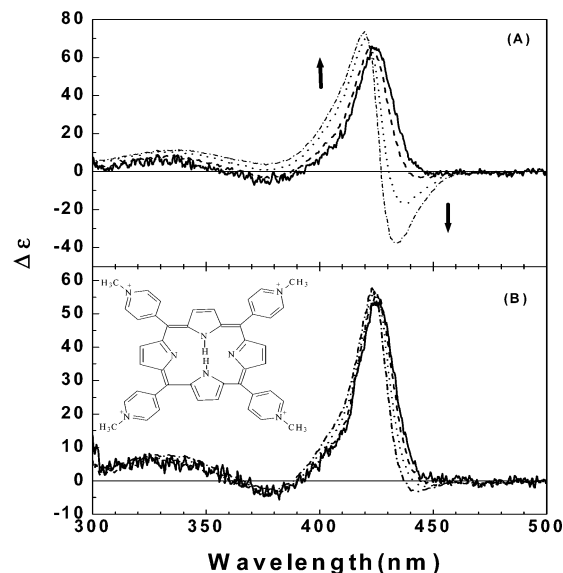


**Figure 1.** Representative CD spectra of TMPyP in the presence of d(A)<sub>12</sub>·d(T)<sub>12</sub> duplex (A) and d(A)<sub>12</sub>·[d(T)<sub>12</sub>]<sub>2</sub> triplex (B) at 4 °C. [oligonucleotide] = 5 μM. The mixing ratios are 0.4, 1.0, 2.0, and 3.0. 1.0 mM cacodylate buffer pH 7.0 containing 20 mM NaCl and 1 mM Mg<sup>2+</sup> (for triplex) was used in this work.

at 420 nm were apparent in the duplex–TMPyP complex case (Figure 1, panel A). Similar CD spectra for the poly(dA)·poly(dT)–TMPyP complex were reported.<sup>3</sup> This characteristic bisignate CD spectrum has been assigned to the formation of the porphyrin exciton or the assembly of porphyrin on the DNA template.<sup>3,4</sup> By comparing Figure 1A and B, it is clear that the stacked or assembled TMPyP, which produces the excitonic CD band, is located at the major groove because the excitonic CD was not apparent when the major groove of the d(A)<sub>12</sub>·d(T)<sub>12</sub> duplex was blocked by the third d(T)<sub>12</sub> strand. An isodichroic point observed near 423 nm, between excitonic and monomeric TMPyP, indicates that the transition occurs between these two states. The decrease in monomeric TMPyP near the minor groove seems to be related to the formation of the excitonic porphyrin.

When the mixing ratio increased further, the intensity of the exciton CD of TMPyP complexed with the d(A)<sub>12</sub>·d(T)<sub>12</sub> duplex increases: it reaches a maximum at the mixing ratio of 4.0, which corresponds to 1 TMPyP molecule per 3 base pairs or 6 nucleobases (Figure 2A, and inset). A similar behavior in the excitonic CD in the Soret band for the poly(dA)·poly(dT)–TMPyP complex was reported.<sup>3</sup> In the d(A)<sub>12</sub>·[d(T)<sub>12</sub>]<sub>2</sub>–TMPyP complex case, the excitonic behavior is pronounced at a much higher mixing ratio, starting at 4.0 (Figure 2B), which corresponds to 1 TMPyP per 3 base triplets. This observation again indicates that the formation of the TMPyP exciton at a mixing ratio lower than 4.0 is inhibited

<sup>†</sup> Yeungnam University.

<sup>‡</sup> Korea Institute of Science and Technology.

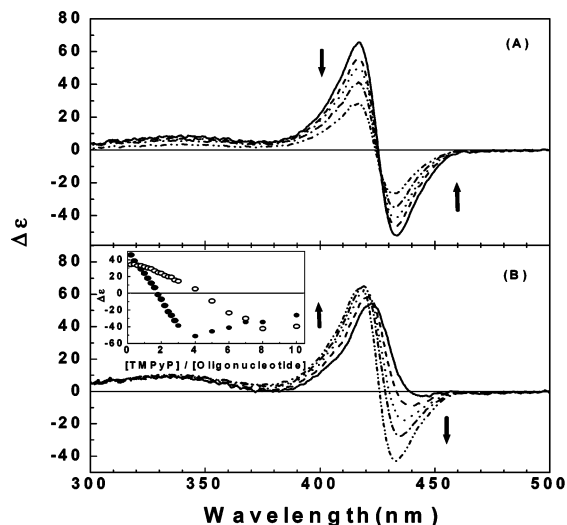


**Figure 2.** CD spectrum of TMPyP in the Soret band in the presence of  $d(A)_{12} \cdot d(T)_{12}$  duplex (A) and  $d(A)_{12} \cdot [d(T)_{12}]_2$  triplex (B) at 4 °C at the higher ratios. In the arrow direction, [TMPyP]/[oligonucleotide] ratios are 3.0, 4.0, 5.0, 7.0, and 10.0. [oligonucleotide] = 5  $\mu$ M.

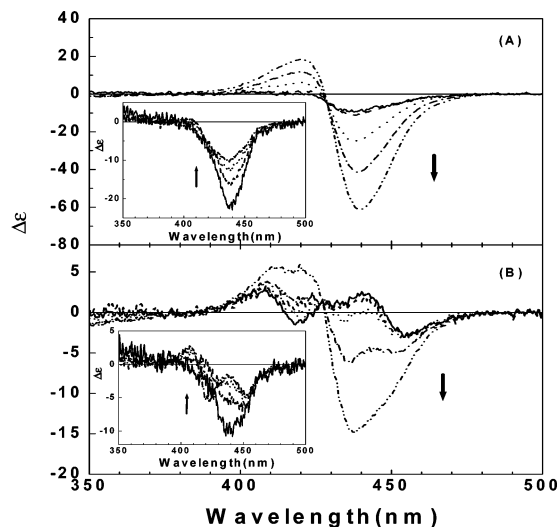


**Figure 3.** CD spectrum of TMPyP in the Soret band in the presence of  $d(G)_{12} \cdot d(C)_{12}$  duplex (A) and  $d(G)_{12} \cdot d(C)_{12} \cdot d(C)_{12}^+$  triplex (B) at 4 °C. In the arrow direction, the mixing ratios are 1.0, 1.6, 2.0, 2.4, and 3.0. [oligonucleotide] = 5  $\mu$ M. Inset: at low mixing ratios of 0.2, 0.4, 0.6, and 0.8.

by the presence of the third strand. As the concentration of TMPyP increases, the equilibrium shifts toward the stacking of TMPyP in the major groove of duplex oligonucleotides; that is, the third  $d(T)_{12}$  strand is removed by the population of TMPyP.

Induced CD spectra of TMPyP in the Soret region in the presence of  $d(G)_{12} \cdot d(C)_{12} \cdot d(C)_{12}^+$  triplex and  $d(G)_{12} \cdot d(C)_{12}$  duplex are depicted in Figure 3, with the same ionic strength as that in the AT case but at pH 5.0, which is required to stabilize the triplex. At the binding ratio of 0.2, negative CD bands were apparent for both the duplex and the triplex complex (Figure 3, inset), which is diagnostic of intercalation.<sup>2e,4b,9</sup> In the duplex case (Figure 3A), the magnitude of this negative band at 436 nm decreases as the mixing ratio increases, which may reflect the relatively low binding constant of TMPyP. Between the mixing ratio of 1.0–1.6, the shape

of the CD band remains. A further increase in the mixing ratio results in a bisignate CD band with a negative band at 440 nm and positive band at 420 nm, which is typical for the TMPyP stacked outside of DNA. On the other hand, the intensity of the negative band of the TMPyP- $d(G)_{12} \cdot d(C)_{12} \cdot d(C)_{12}^+$  triplex complex at a very low mixing ratio is one-half that in the duplex and starts to disappear at the mixing ratio as low as 0.4. The extrusion of intercalated TMPyP is probably due to repulsion of the positive charges of TMPyP and protonated cytosines. In the intermediate mixing ratios (0.8–2.0), the shape of the CD band seems to be a combination of two excitonic CD. As the mixing ratio increases further, the excitonic bisignate CD appears, which resembles that of the AT case. At extremely high mixing ratios, the magnitude of the excitonic CD is comparable to that of the duplex complex (data not shown). Although a full understanding of the porphyrin species at an intermediate mixing ratio requires more investigation, it is clear that the formation of bisignate CD is inhibited by the presence of the third strand. This result demonstrates that the location of the stacked porphyrin in the  $d(G)_{12} \cdot d(C)_{12}$  duplex is also the major groove.

In conclusion, the third strand in the triplex inhibits the formation of the TMPyP assembly. Therefore, TMPyP stacking occurs in the major groove of both the  $d(A)_{12} \cdot d(T)_{12}$  and the  $d(G)_{12} \cdot d(C)_{12}$  duplexes.

**Acknowledgment.** This work was supported by the Korea Science and Engineering Foundation (R01-2003-000-00043-0).

## References

- (1) (a) Pasternack, R. F.; Gibbs, E. J. In *Metal Ions in Biological Systems*; Sigel, A., Sigel, H., Eds.; Marcel Dekker: New York, 1996; pp 367–397. (b) Fiel, R. J. *J. Biomol. Struct. Dyn.* **1990**, *6*, 3093–3118. (c) Marzilli, L. G. *New J. Chem.* **1990**, *14*, 409–420.
- (2) (a) Kuroda, R.; Tanaka, H. *J. Chem. Soc., Chem. Commun.* **1994**, 1575–1576. (b) Schnier, H.-J.; Wang, M. *J. Org. Chem.* **1994**, *59*, 7473–7478. (c) Sehlstedt, U.; Kim, S. K.; Carter, P.; Goodisman, J.; Vollano, J. F.; Nordén, B.; Dabrowiak, J. C. *Biochemistry* **1994**, *33*, 417–426. (d) Yun, B. H.; Jeon, S. H.; Cho, T.-S.; Yi, S. Y.; Sehlstedt, U.; Kim, S. K. *Biophys. Chem.* **1998**, *70*, 1–10. (e) Lee, Y.-A.; Lee, S.; Cho, T.-S.; Kim, C.; Han, S. W.; Kim, S. K. *J. Phys. Chem. B* **2002**, *106*, 11351–11355.
- (3) Lee, S.; Jeon, S. H.; Kim, B.-J.; Han, S. W.; Jang, H. G.; Kim, S. K. *Biophys. Chem.* **2001**, *92*, 35–43.
- (4) (a) Marzilli, L. G.; Banville, L. D.; Zon, G.; Wilson, W. D. *J. Am. Chem. Soc.* **1986**, *108*, 4188–4192. (b) Hui, X. W.; Gresh, N.; Pullman, B. *Nucleic Acids Res.* **1990**, *18*, 1109–1114. (c) Ford, K. G.; Neidle, S. *Bioorg. Med. Chem.* **1995**, *6*, 671–677. (d) Guliaev, A. B.; Leontis, N. B. *Biochemistry* **1999**, *38*, 15425–15437.
- (5) (a) Carvlin, M. J.; Datta-Gupta, N.; Fiel, R. J. *Biochem. Biophys. Res. Commun.* **1982**, *108*, 66–73. (b) Pasternack, R. F.; Gibbs, E. J.; Villafranca, J. J. *Biochemistry* **1983**, *22*, 5409–5417. (c) Pasternack, R. F.; Gibbs, E. J.; Villafranca, J. J. *Biochemistry* **1983**, *22*, 2406–2414. (d) Pasternack, R. F.; Brigandi, R. A.; Abrams, M. J.; Williams, A. P.; Gibbs, E. J. *Inorg. Chem.* **1990**, *29*, 4483–4486. (e) Pasternack, R. F.; Gibbs, E. J.; Collings, P. J.; dePaula, J. C.; Turzo, L. C.; Terracina, A. *J. Am. Chem. Soc.* **1998**, *120*, 5873–5878. (f) Strickland, J. A.; Marzilli, L. G.; Gay, K. M.; Wilson, W. D. *Biochemistry* **1988**, *27*, 8870–8878.
- (6) (a) Kim, S. K.; Nordén, B. *FEBS Lett.* **1993**, *315*, 61–64. (b) Tuite, E.; Nordén, B. *J. Chem. Soc., Chem. Commun.* **1995**, 53–54.
- (7) (a) Kim, H. K.; Kim, J.-M.; Kim, S. K.; Rodger, A.; Nordén, B. *Biochemistry* **1996**, *35*, 1187–1194. (b) Choi, S.-D.; Kim, M.-S.; Kim, S. K.; Lincoln, P.; Tuite, E.; Nordén, B. *Biochemistry* **1997**, *36*, 214–223. (c) Kim, S. K.; Sun, J.-S.; Garestier, T.; Hélène, C.; Nguyen, C. H.; Bisagni, E.; Rodger, A.; Nordén, B. *Biopolymers* **1997**, *42*, 101–111. (d) Cho, C. B.; Cho, T.-S.; Kim, S. K.; Kim, B.-J.; Han, S. W.; Jung, M.-J. *Bull. Korean Chem. Soc.* **2000**, *21*, 995–999. (e) Cho, C.-B.; Jung, K.-S.; Kim, J. H.; Cho, T.-S.; Jang, H. G.; Kim, S. K. *Biochim. Biophys. Acta* **2001**, *1517*, 220–227.
- (8) Ismail, M. A.; Rodger, P. M.; Rodger, A. *J. Biomol. Struct. Dyn.* **2000**, *Conversations 11*, 335–348.
- (9) Lee, S.; Lee, Y.-A.; Lee, H. M.; Lee, J. Y.; Kim, D. H.; Kim, S. K. *Biophys. J.* **2002**, *83*, 371–381.

JA034499J